Shape Optimization of a Plate-Fin Type Heat Sink with Triangular-Shaped Vortex Generator

Kyoungwoo Park*, Dong-Hoon Choi

The Center of Innovative Design Optimization Technology, Hanyang University (HIT Rm # 312), 17 Haengdang-dong, Sungdong-gu, Seoul 133-791, Korea

In this study the optimization of plate-fin type heat sink with vortex generator for the thermal stability is performed numerically. The optimum solutions in the heat sink are obtained when the temperature rise and the pressure drop are minimized simultaneously. Thermal performance of heat sink is influenced by the heat sink shape such as the base-part fin width, lower-part fin width, and basement thickness. To acquire the optimal design variables automatically, CFD and mathematical optimization are integrated. The flow and thermal fields are predicted using the finite volume method. The optimization is carried out by means of the sequential quadratic programming (SQP) method which is widely used for the constrained nonlinear optimization problem. The results show that the optimal design variables are as follows ; B_1=2.584 mm, B_2= 1.741 mm, and t=7.914 mm when the temperature rise is less than 40 K. Comparing with the initial design, the temperature rise is reduced by 4.2 K, while the pressure drop is increased by 9.43 Pa. The relationship between the pressure drop and the temperature rise is also presented to select the heat sink shape for the designers.

Key Words : Design Optimization, Plate-Fin Heat Sink, Vortex Generator, CFD, SQP Method

Nomenclature

B_1, B_2 : Base- and lower-part of fin [m]
B : Matrix in Eq. (24)
c_P : Specific heat at constant pressure [J/kgK]
C_1, C_2, C_3, C_λ, C_μ : Empirical constants in the k-ε model
f_R, f_λ : Empirical functions in the k-ε model
$F(\mathbf{X})$: Objective function
g_i : Acceleration of gravity [m/s^2]
$g_j(\mathbf{X})$: Inequality constraints
G_b, G_k : Generation terms in the k-ε equations
h : Fin height [m]
$h_i(\mathbf{X})$: Equality constraints
H : Height of heat sink ($=h+t$), [m]
H : Hessian matrix
k : Turbulent kinetic energy [m^2/s^2]
k_s : Thermal conductivity of solid [W/m·K]
L : Length of heat sink [m]
L_h : Length of heat source [m]
P : Pressure [Pa]
ΔP : Pressure drop [Pa]
Pr : Prandtl number
Q : Dissipated heat [W]
R : Reynolds number
S : Fin-to-fin spacing [m]
S : Search direction in Eq. (20)
t : Basement thickness of heat sink [m]
T, T' : Mean and fluctuating temperature, respectively [K]
ΔT : Temperature rise [K]
u_j, u_j' : Mean and fluctuating velocities, respectively [m/s]
W : Width of heat sink [m]

* Corresponding Author,
E-mail : kwoopark@hanyang.ac.kr
TEL : +82-2-2290-1639; **FAX** : +82-2-2291-4070
The Center of Innovative Design Optimization Technology, Hanyang University (HIT Rm # 312), 17 Haengdang-dong, Sungdong-gu, Seoul 133-791, Korea.
(Manuscript **Received** February 20, 2004; **Revised** June 24, 2004)

W_h : Width of heat source [m]
x, y, z : Cartesian coordinates [m]
$\mathbf{X}$: Design variable vector

Greek symbols

α : Step length parameter in Eq. (20)
α_t : Eddy diffusivity for heat [m^2/s]
β : Thermal expansion coefficient [1/K]
δ_{ij} : Kronecker delta
ε : Dissipation rate of k [m^2/s^3]
ϕ : General dependent variable
μ, μ_t : Viscosity and eddy viscosity [$N \cdot s/m^2$]
θ_j : Thermal resistance [K/W] in Eq. (16)
ρ : Density [kg/m^3]
$\sigma_k, \sigma_\varepsilon$: Turbulent Prandtl and Schmidt number for k and ε

Subscripts

in : Inlet
j : Junction or maximum
k : Number of iteration
∞ : Ambient

1. Introduction

For higher thermal performance of the plate-fin heat sink, the internal forced convection cooling technique has been widely employed in thermal systems. Recently, the use of vortex generator is one of the popular means for improvement of cooling effect because electronic devices have become more compact and hence dissipated more heat. Artificial roughness on a flow passage retards the development of thermal boundary layer and creates the local wall turbulence due to flow separation and reattachment, thus greatly enhancing the heat transfer rate. However, it also leads to higher pressure loss in a channel. In addition, the size of heat exchangers is determined according to the limited space they are to be installed in. Therefore, heat exchangers must be designed by considering the pressure drop and the available space as well as the thermal performance. For this reason, the importance of numerical optimization in the design of heat sink has been emphasized.

In recent years, many algorithms for numerical optimization technologies have been proposed in order to offer a logical approach to design automation. In addition, as the physical phenomena considered in industrial applications become more complicated, the use of commercial CFD (computational fluid dynamics) codes is dramatically increased. Therefore, the combined field of computational flow/thermal optimization has been receiving much attention due to advances in both the fields of computational fluid dynamics/heat transfer and computer aided optimization (CAO). In practical situations, it is very difficult to combine commercial CFD solvers with mathematical optimization methods because all of the commercial CFD codes solve the flow and thermal characteristics on the GUI (graphical user interface). Recently, Park et al.(2004) studied the design optimization of the plate-fin and tube heat exchanger. They integrated the FLUENT, which is a commercial CFD code, and the optimization technology in order to propose the optimum design variables of a heat exchanger. Ryu et al.(2003) developed the program for predicting the thermal performance of a complex micro-channel heat sink and applied it to optimize the heat sink.

Augmentation of the thermal performance of heat sink with vortex generator has been receiving considerable attention for many years because of its importance over a wide range of industrial applications. Yuan et al.(1998) predicted the forced convection heat transfer in parallel-plate channels having streamwise-periodic rod disturbances on its two principal walls in the Reynolds number range of 50−700. They concluded that the effect of rod disturbances can increase the heat transfer by four times greater than that of a smooth channel, with the penalty of a much greater pressure drop. Experimental and numerical studies were conducted to investigate the forced convection and fluid friction of a turbulent airflow in a horizontal air-cooled rectangular duct with square-sectioned cross-ribs by Wong et al.(2003). They concluded that use of cross-ribs could be a promising solution to enhance heat transfer and the major drawback of applying the cross-ribbed surface was the larger pressure drop.

Much research on the optimization of heat sink has been conducted. However, most of them have focused on the parametric study which influences the flow and thermal characteristics for obtaining the optimum design. Ledezma and Bejan (1996) performed the study on the cooling performance of plate-fin heat sink by means of numerical and experimental methods. They argued that the thermal performance of heat sink increases when fins are arranged with inclined angle and the velocity of coolant increases. Jang et al. (1996) studied the flow and heat transfer over a multi-row plate-pin and tube heat exchanger. They concluded that the average heat transfer coefficient and the pressure drop of a staggered array are 15-27% and 20-25% higher than those of an in-lined array, respectively. Wirtz and Zcheng (1998) have described a methodology for determining an optimum fin configuration for the fan-driven heat sink. They also insisted that the knowledge of both the assembly fan characteristics and the heat transfer/pressure drop characteristics of the heat sink are required for proper design.

Although the aforementioned researches can be useful in designing a heat sink, they proposed the correlation equations for the optimum design variables by considering only the flow and thermal characteristics of heat sink. It means that most of previous works carried out optimization without considering the mathematical optimization technique. It is also very difficult to find works for the optimization of plate-fin type heat sink to enhance the thermal performance. Therefore, in this work, in order to obtain the optimal values of the design variables of plate-fins heat sink, we combined the CFD with the CAO technologies. For the mathematical optimization, the SQP (sequential quadratic programming) method is applied.

2. Physical Model

The thermal system under consideration for optimization of heat sink is illustrated schematically in Fig. 1. It consists of three parts : duct, heat sink, and reactor as shown in Fig. 1. The

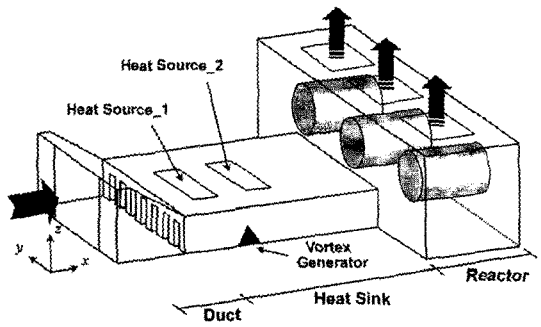

Fig. 1 Schematic diagram of thermal system and coordinate system

isothermal coolant air induced by axial fan (Model : 3112KL-05W-B50, Size : 32×80×80 mm, Max. flow rate : 1.46 m^3/min) passes the duct which plays a role of flow guidance and enters the flow passages between fins of the plate-fin type heat sink. Finally, a heated air flows out through exits located top wall of the reactor after it cools the heat sink.

Figure 2 depicts the detailed physical configuration of the plate-fins heat sink schematically because the optimization problem considered in this study is to maximize the thermal performance of the fan-driven heat sink. The heat sink is made of aluminum (ρ=2,707 kg/m^3, k_s=204 W/mK) and is fabricated by extruding fins. The overall dimensions of heat sink are a length L=430 mm, a width of W=188 mm, and a height of H=60 mm. Noting that the height of the heat sink (H) is the sum of the fin height (h) and base thickness of heat sink (t). Two heat sources with projected heating areas (dimension of 62×122 mm, L_h×W_h) mounted on the top wall surface of heat sink uniformly generate the heat by two different electric resistance heaters (Q_1=348 W, Q_2=321 W) as shown in Fig. 2. A full-span vortex generator perpendicularly to the flow direction is mounted on the bottom wall of heat sink and it is located between two heat sources. A vortex generator has a triangular cross-section. The heat generated by heat sources is conducted through the heat sink at first and then it is rejected from the heat sink to the environment by means of forced convection. Thus, the problem considered becomes a conjugated heat transfer problem. Figure 2 also shows

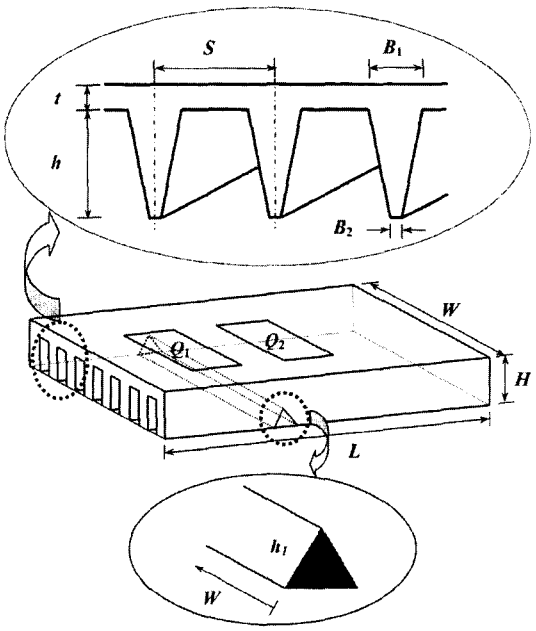

Fig. 2 Plate-fin type heat sink

that the internal shape of heat sink can be determined by geometrical parameters such as the fin pitch (S) or number of fins (n), basement thickness of heat sink (t) or fin height (h), base part fin width (B_1), and lower part fin width (B_2).

Generally speaking, the optimization refers to find the design variables with the minimized objective function numerically. In this case, the design variables are commonly subjected to the constraint conditions. Thus, the nonlinear, constrained optimum design problem can be expressed mathematically as follows:

Find

$$\mathbf{X}=\{x_1, x_2, \cdots, x_N\}^T \tag{1}$$

to minimize

$$F(\mathbf{X}) \tag{2}$$

subject to

$$g_j(\mathbf{X}) \leq 0 \text{ for } j=1, M \tag{3a}$$

$$h_i(\mathbf{X}) = 0 \text{ for } i=1, M \tag{3b}$$

$$\mathbf{X}_i^L \leq \mathbf{X}_i \leq \mathbf{X}_i^U \text{ for } i=1, N \tag{3c}$$

where $\mathbf{X}$ represents the design variable vector and N is the number of design variables with $N=3$ in this study. $F(\mathbf{X})$ is the objective function which depends on the values of the design variables. $g_j(\mathbf{X})$ and $h_i(\mathbf{X})$ denote the inequality and equality constraints, respectively. $\mathbf{X}_i^L$ and $\mathbf{X}_i^U$ are the lower and upper limits of the design variables, respectively, and they simply limit the region of search for the optimization. M is the number of constraints.

To optimize the shape of heat sink for high thermal performance, the thermal resistance and the pressure drop, which can be predicted by the calculation of flow and thermal fields, are minimized simultaneously. Therefore, it is very important to understand the flow and thermal characteristics in the heat sink for optimization.

3. Numerical Modeling

3.1 Flow and thermal fields

3.1.1 Mean flow equations

The physical problem considered in this study is the three-dimensional turbulent mixed convective flow of steady and incompressible fluid. The fluid properties are taken to be constant except for the density in the buoyancy terms of the momentum equation. The effects of viscous dissipation and radiation heat transfer are assumed to be negligibly small. Due to the symmetric geometry, the computation is only carried out one half of the physical domain. Using the above-mentioned assumptions, the time-averaged governing equations for mass, momentum, and energy can be expressed in Cartesian tensor form as follows:

Continuity:

$$\frac{\partial(\rho u_j)}{\partial x_j}=0 \tag{4}$$

Momentum:

$$\frac{\partial(\rho u_i u_j)}{\partial x_j} = -\frac{\partial P}{\partial x_i}+\frac{\partial}{\partial x_j}\left[\mu\left(\frac{\partial u_i}{\partial x_j}+\frac{\partial u_j}{\partial u_i}\right)-\overline{\rho u_i' u_j'}\right]+\rho g_i \tag{5}$$

Energy:

• for liquid:

$$\frac{\partial(\rho u_j T)}{\partial x_j} = \frac{\partial}{\partial x_j}\left(\frac{\mu}{\mathrm{Pr}}\frac{\partial T}{\partial x_j}-\overline{\rho u_i' T'}\right)+S_\phi \tag{6}$$

• for solid :

$$\frac{\partial}{\partial x_i}\left(k_s\frac{\partial T}{\partial x_i}\right)+\dot{q}=0 \tag{7}$$

where $i=1$, 2 and 3 denote x, y, and z directions, respectively. The term S_ϕ in Eq. (6) stands for the appropriate source of temperature T and it is the rate of heat release. $\dot{q}$ is the rate of heat generation per unit volume in the conduction equation of Eq. (7).

3.1.2 Turbulent modeling equations

In Eqs. (5) and (6), the Reynolds stress, $\overline{\rho u_i' u_j'}$, and the turbulent heat flux, $\overline{\rho u_i' T'}$, which govern the turbulent diffusion, should be determined. Using the eddy viscosity approximation, they are defined as follows :

$$-\overline{\rho u_i' u_j'}=\mu_t\left(\frac{\partial u_i}{\partial x_j}+\frac{\partial u_j}{\partial x_i}\right)+\frac{2}{3}k\delta_{ij}$$
$$-\overline{\rho u_i' T'}=\alpha_t\frac{\partial T}{\partial x_i} \tag{8}$$

where μ_t and α_t are the turbulent (or eddy) viscosity and the eddy diffusivity for heat, respectively. They are computed as

$$\mu_t=\rho C_\mu\frac{k^2}{\varepsilon}$$
$$\alpha_t=C_\lambda f_\lambda k\left(\frac{k}{\varepsilon}\right)^n\left(\frac{\overline{T'^2}}{\varepsilon_t}\right)^m \tag{9}$$
$$n+m=1$$

where C_λ, f_λ denote the model constant and function including the near wall effect in thermal field. To obtain the eddy viscosity and eddy diffusivity, the closure problem of the governing equations has to be resolved. Thus, the standard $k-\varepsilon$ turbulence model (Rodi, 1984) is introduced in this work. According to the eddy-viscosity concept, the turbulent kinetic energy (k) and its dissipation rate (ε) are obtained from the following transport equations :

$$\frac{\partial(\rho u_j k)}{\partial x_j}=\frac{\partial}{\partial x_j}\left[\left(\mu+\frac{\mu_t}{\sigma_k}\right)\frac{\partial k}{\partial x_i}\right]+G_k+G_b-\rho\varepsilon \tag{10}$$

$$\frac{\partial(\rho u_j\varepsilon)}{\partial x_j}=\frac{\partial}{\partial x_j}\left[\left(\mu+\frac{\mu_t}{\sigma_\varepsilon}\right)\frac{\partial\varepsilon}{\partial x_i}\right]+C_1\frac{\varepsilon}{k}(G_k+C_3G_b)-C_2\rho\frac{\varepsilon^2}{k} \tag{11}$$

In Eqs. (10) and (11), G_k and G_b are the turbulent production terms of stress and buoyancy force, respectively, and are given by

$$G_k=-\overline{\rho u_i' u_j'}\left(\frac{\partial u_i}{\partial x_j}\right),\quad G_b=g_i\beta\frac{\mu_t}{\sigma_t}\frac{\partial T}{\partial x_i} \tag{12}$$

β is the thermal expansion coefficient and is given by $-1/\rho$ for ideal gases. The model constants and various functions used in the $k-\varepsilon$ model are as follows (Rodi, 1984 ; Abe et al., 1996) :

$$C_\mu=0.09,\ C_1=1.44,\ C_2=1.92,\ \sigma_k=1.0,\ \sigma_\varepsilon=1.3,$$
$$C_3=\tanh\left|\frac{v}{u}\right|,\ C_\lambda=0.1$$
$$f_R=\left[1-\exp\left(-\frac{R_\varepsilon}{16}\right)\right]^2\left[1+\frac{3}{R_t^{3/4}}\right] \tag{13}$$
$$R_\varepsilon=\frac{y(\nu\varepsilon)^{1/4}}{\nu},\quad R_t=\frac{k^2}{\nu\varepsilon}$$

3.1.3 Boundary conditions

We use the following boundary conditions to predict the flow and thermal fields in thermal system including the heat sink.

Inlet : The coolant of a constant temperature ($T_{in}=318$ K) induced by axial fan enters the system with a constant velocity ($u_{in}=1.27$ m/s) and a swirl condition of 60 rad/s. The corresponding turbulent kinetic energy and its dissipation rate are calculated from the following formula : $k_{in}=15I_0^2u_{in}^2$, $\varepsilon_{in}=k_{in}^{3/2}/L_\varepsilon$, where the local turbulence intensity, I_0 is assumed to be 0.1 and L_ε is a length scale for dissipation, taken here as 80 mm (fan width).

Outlet : Pressure boundary condition is imposed at the outflow plane. For the other variables, the Newmann condition is employed.

Solid surfaces : A no-slip boundary condition for all solid walls is assigned for velocity. For the turbulent kinetic energy and its dissipation rate, the wall function based on empirical wall law is employed. At the heat sink walls, the following thermal boundary conditions are imposed ; Two different heat ($Q_1=348$ W and $Q_2=321$ W) are uniformly applied to the heat sink at the top wall of heat sink (122×62 mm) by two heat sources. At the side wall and the top wall except for heat

sources, the convective boundary condition is used (h=3 W/m^{2}K). At the bottom wall of heat sink, adiabatic condition is adopted. The solid walls of the duct and reactor are assumed to be adiabatic.

Symmetric plane: The symmetric conditions are imposed for all dependent variables at the plane of symmetry (i.e., y=0).

3.1.4 Numerical solution procedure

The governing equations for three dimensional turbulent flow and thermal fields are solved using FLUENT which is a commercial finite volume CFD code (FLUENT, 1998). The reason for using the CFD code is as follows: to obtain the optimum design variables by means of the mathematical optimization technique, a fast and reliable computer program must be used because it operates repeatedly for many different geometrical configurations during the optimization process. All of the commercial CFD codes, however, basically solve the flow and thermal characteristics on the GUI. Thus, it is an important task to combine commercial CFD solvers with mathematical a optimization method in order to carry out the optimization automatically. The SIMPLE algorithm (Patankar, 1980) is used to calculate the pressure correction equation in the momentum equation. The power law scheme is employed for the treatment of convection and diffusion terms.

In the optimization problem, because a new shape of fins is proposed in every iterative step of the optimization process, a new grid system according to the modified design variables is required. Therefore, the number of cells for the computational domain has to be given sufficiently large (for baseline geometry, its number is around 1,300,000 cells) by considering the fine grid system at the solid-gas interfaces.

When the results satisfy the following conditions simultaneously, the solutions are treated as converged ones:

$$R=\sum_{domain}|a_{nb}\phi_{nb}+b-a_P\phi_P|<10^{-5} \quad (14a)$$

$$\left|\frac{\phi_{k+1}-\phi_k}{\phi_k}\right|<10^{-5} \quad (14b)$$

where R represents the residual sum and ϕ is a general dependent. The subscripts i and nb are the number of iteration and the neighborhood grid points, respectively.

3.2 Numerical optimization

3.2.1 Objective functions and design variables

The improvement of heat sink performance can be easily achieved both by extending the heat transfer area and by using a material of higher thermal conductivity. Increasing the heat transfer area, however, results in increasing the pressure drop for a given fan operating condition. This means that it is very important to understand the mechanisms that influence the heat transfer and pressure drop of the plate-fins heat sink. Thus, to maximize the thermal performance of a plate-fins heat sink, the heat sink configuration and its array should be optimized.

For a fixed volume of heat sink, a high thermal performance (or cooling efficiency) can be achieved when the thermal resistance and the pressure drop are minimized, simultaneously. Generally, the objective functions to be minimized are the pressure drop (ΔP) and the junction-to-ambient thermal resistance (θ_j) and they are defined as

$$\theta_j=\frac{T_j-T_\infty}{Q},\ \Delta P=P-P_\infty \quad (16)$$

where T_j is the junction temperature, T_∞ the ambient temperature, and Q the heat generated through the heat sink. P and P_∞ are the average pressure in the heat sink and the ambient pressure, respectively.

In practical situation, however, the maximum temperature at the junction of heat source and heat sink surface (T_j or T_{max}) should be maintained under the desired temperature. For this, we use the maximum temperature as one of the constraint conditions instead of using the objective function. Thus, in this study the pressure drop is adopted as the objective function only.

The geometric parameters which strongly influence the thermal performance of the heat sink

are the base-width of fin (B_1), lower-width of fin (B_2), and basement thickness of heat sink (t). Thus, three design variables are considered in this study, that is, $x_1=B_1$, $x_2=B_2$, and $x_3=t$ ($\mathbf{X}=[B_1, B_2, t]$).

3.2.2 SQP method

Various computational algorithms have been proposed to solve the nonlinear optimization problem with constrained functions. Optimization problem of Eqs. (1)-(3) is solved by means of the sequential quadratic programming (SQP) method (Vanderplaats, 1984) in this study. The SQP method is a gradient-based optimization algorithm and has been turned out as one of the most efficient algorithms for solving the small sized nonlinear constrained optimization problem like this study.

In typical gradient based optimization algorithm, an iterative improvement is carried out over successive designs until an optimal design is achieved. From this point of view, the gradients of objective functions are calculated using the finite difference method (FDM) to minimize them. In this study, the size of perturbation (or step-size) of 1×10^{-3} is used according to the results of the sensitivity analysis for the objective function and constraints. The design variables are updated by the following equation

$$\mathbf{X}_{k+1}=\mathbf{X}_k+\alpha_k\cdot\mathbf{S}_k \tag{20}$$

In Eq. (20), the search direction, $\mathbf{S}$, and the step length parameter, α, which minimizes the objective function, should be determined in order to complete the optimization process. Most of optimization algorithms determine the search direction by means of the gradient method and then, precede the one-dimensional search in order to improve the design variables for the selected direction. However, initial value of α for the one-dimensional search is usually given by arbitrary one. Therefore, to obtain the convergence solutions, the choice of initial value of α is very important.

To obtain the search direction, we use the SQP method. The basic concept of the SQP method is as follows: the objective function is expanded in a second order Taylor series at the current values of the design variables, while the constraints are linearized by means of a first order Taylor series expansion.

First, the SQP method linearizes the objective function and the constrained condition as follows;

Minimize

$$F(\mathbf{X}_{k+1})=F(\mathbf{X}_k)+\nabla F(\mathbf{X}_k)^T\mathbf{S}_k \tag{21}$$

subject to

$$g_j(\mathbf{X}_{k+1})=g_j(\mathbf{X}_k)+\nabla g_j(\mathbf{X}_k)^T\mathbf{S}_k\le0 \tag{22a}$$

$$h_i(\mathbf{X}_{k+1})=h_i(\mathbf{X}_k)+\nabla h_i(\mathbf{X}_k)^T\mathbf{S}_k=0 \tag{22b}$$

And then, the search direction is determined by introducing the following quadratic approximated objective function,

Minimize

$$Q(\mathbf{S}_{k+1})=F(\mathbf{X}_k)+\nabla F(\mathbf{X}_k)^T\mathbf{S}_k+\frac{1}{2}(\mathbf{S}_k)^T\mathbf{B}\mathbf{S}_k \tag{23}$$

The linearized objective function, constrained condition, and quadratic approximated objective function, as shown in Eqs. (21)-(23), are calculated using the modified method of feasible direction (MMFD). The matrix $\mathbf{B}$, which is a unit matrix initially, is a positive definite matrix. Once the one-dimensional search is completed, the following BFGS (Broydon-Fletcher-Goldfarb-Shanno) method is used for updating the matrix $\mathbf{B}$ in this study.

$$\mathbf{B}^*=\mathbf{B}-\frac{\mathbf{B}\mathbf{S}\mathbf{S}^T\mathbf{B}}{\mathbf{S}^T\mathbf{B}\mathbf{S}}+\frac{\eta\eta^T}{\mathbf{S}^T\eta} \tag{24}$$

where

$$\begin{gathered}\mathbf{S}=\mathbf{X}_{k+1}-\mathbf{X}_k,\ \eta=\theta\mathbf{Y}+(1-\theta)\mathbf{B}\mathbf{S}\\ \mathbf{Y}=\nabla_X\Phi_{k+1}-\nabla_X\Phi_k\\ \Phi_k=F(\mathbf{X})+\sum_{j=1}^{M}\lambda_j g_j(\mathbf{X})\end{gathered} \tag{25}$$

$$\theta=\begin{cases}1.0 & \text{if}\quad \mathbf{S}^T\mathbf{Y}\ge0.2\mathbf{S}^T\mathbf{B}\mathbf{S}\\ \dfrac{0.8\mathbf{S}^T\mathbf{B}\mathbf{S}}{\mathbf{S}^T\mathbf{B}\mathbf{S}-\mathbf{S}^T\mathbf{Y}} & \text{if}\quad \mathbf{S}^T\mathbf{Y}\ge0.2\mathbf{S}^T\mathbf{B}\mathbf{S}\end{cases}$$

After $\mathbf{B}^*$ replaces $\mathbf{B}$ and a new iteration is commenced.

When the difference between the successive values of the objective function, $F(\mathbf{X})$, satisfies the following convergence criterion, the optimization process terminates :

$$|F(\mathbf{X}_{k+1}) - F(\mathbf{X}_k)| \leq \varepsilon_a \tag{26}$$

where ε_a is a specified tolerance and is set to $\varepsilon_a = 10^{-4}$.

4. Numerical Methodology

In order to obtain the optimal design parameters of the heat exchanger with plate-fins, the following three programs are used ;

(1) the main program which defines various arrays and parameters,

(2) the analyzer that evaluates the objective functions (i.e., program for predicting the flow and thermal fields), and

(3) the optimizer which can solve a nonlinear optimization problem.

Figure 3 shows the numerical methodology for optimization. Once the objective functions (θ_j and Δp) are obtained as the results of calculation of flow and thermal fields by the analyzer, the main program calls the optimizer to proceed with optimization. The optimizer may modify the design variables. When the optimizer requires new values of the objective functions, it returns to the main program and the analyzer is called to calculate them. In this step, the analyzer should generate a new grid system because new design variables are proposed by the optimizer. This process is repeated until the optimization is complete and is performed automatically. As a result of optimization, the optimal design variables and the corresponding pressure drop and heat transfer rate are obtained.

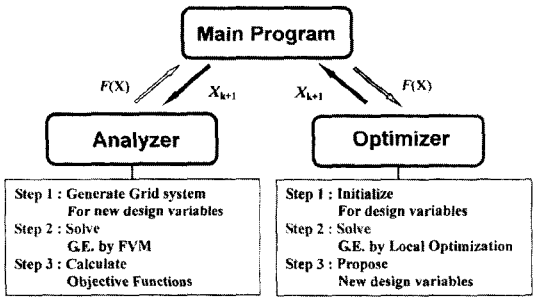

Fig. 3 Numerical methodology for optimization

5. Results and Discussion

The optimization of a plate-fins heat sink with triangular cross-section vortex generator is conducted numerically. The flow and thermal fields for the thermal system including the heat sink are solved by the FLUENT in order to calculate the pressure drop and junction temperature which are chosen as the objective functions. The optimal design variables for minimizing the objective function are obtained by means of the mathematical optimization algorithm, that is, the SQP method.

The baseline geometric parameters and the side constraints for the design variables (B_1, B_2, and t) are shown in Table 1. Overall dimension of heat sink is a $430 \times 188 \times 60$ mm ($L \times W \times H$) base. The fin-to-fin spacing is 7.52 mm and the number of fins is 24. Initially, the fins have a 2 mm width of base-part, 1.5 mm width of lower-part, and a 7 mm of basement thickness, that is, $\mathbf{X}_0 = [B_1, B_2, t ; 2.0, 1.5, 7.0]$. The constraint conditions adopted in this study are as follows ;

Table 1 Geometric parameters of the baseline domain and side constraints for heat sink

Unit : mm

Parameters	Baseline	Side constraints	
		Minimum	Maximum
Length of heat sink, L	430.0	–	–
Width of heat sink, W	188.0	–	–
Height of heat sink, H	60.0	–	–
Fin spacing, s	7.52	–	–
Fin height, h	53.0	35.0	53.0
Base-part fin width*, B_1	2.0	1.25	5.0
Lower-part fin width*, B_2	1.5	1.25	5.0
Base plate thickness*, t	7.0	7.0	25.0

* Design variables

$$\Delta T < \text{specific values, (38 K} - \text{41 K)} \quad (27a)$$

$$B_2/B_1 < 1 \quad (27b)$$

5.1 Effect of vortex generator

First of all, to investigate the effect of vortex generator on the flow and thermal characteristics of heat sink, we compare them for the cases of with and without vortex generator and the results calculated are listed in Table 2. Table 2 presents the maximum temperature (T_j), temperature rise ($\Delta T = T_j - T_\infty$) and pressure drop ($\Delta P$) for two cases. In the table, all operating conditions and geometric configurations are same as the baseline geometry. Vortex generator has a triangular cross section of 20 mm and a width of 188 mm, as shown in Fig. 2. As can be seen in Table 2, for the case of with vortex generator, the maximum temperature is predicted as 362.3 K and is reduced by 4.2 K compared to that of without vortex generator, while the pressure drop is increased from 33.15 Pa to 37.29 Pa. These phenomena can be simply explained by the following two facts: the breaking the thermal boundary layer and the increasing the flow resistance, respectively, by the existence of vortex generator. From the flow and thermal analyses of system, it can be found that the maximum temperature is occurred at the rear-heat source (Heat Source_2, Q_2=321 W). From now on, all results obtained are those of with vortex generator. Table 2 also illustrates that the temperature rise of 44.31 K is exceeded the general desired temperature rise of 40 K which is corresponding to the maximum temperature for safe operating of thermal system. This means that the plate-fin type heat sink must be optimized for the thermal stability.

Table 2 Maximum temperature (T_j) and pressure drop (ΔP) for the cases of with and without vortex generator

	w/o vortex generator	w/ vortex generator
Maximum temperature (T_j)	366.48 K	362.31 K
Temperature rise (ΔT)	48.48 K	44.31 K
Pressure drop (ΔP)	33.15 Pa	37.29 Pa

5.2 Parametric studies

The degree of importance of each design variable is investigated before the design optimization is carried out. That is, the effect of each design variable on the pressure drop and the maximum temperature is examined by varying only one variable among the design variables. Generally, the parametric studies are performed in order to find what the most important design variable in the heat sink performance is and to choose the most appropriate optimization algorithm by analyzing the distribution of design variables.

The junction temperature and pressure drop for various base-part fin widths (B_1) ($1.25 \le B_2 \le 5.0$ mm) are shown in Fig. 4. In this figure, the other design variables are fixed as the baseline geometry such as B_2=1.5 mm and t=7.0 mm ($\mathbf{X}=[B_1, 1.5, 7.0]$). This figure shows that as the base-part fin width increases, the junction temperature decreases, while the pressure drop increases. These phenomena result from the following reasons; for a fixed volume of heat sink ($L \times W \times H$=constant), increasing the B_1 retards the development of the thermal boundary layer. It results in the thinner thermal boundary layer and the larger friction loss due to the increased velocity. Thus, the heat transfer rate and the pressure drop are increased as B_1 is thickened. From these results, it is also found that the optimum value of B_1 may be approximately ranged as $2 < B_1 < 4$ mm, which will also be found in Table 3.

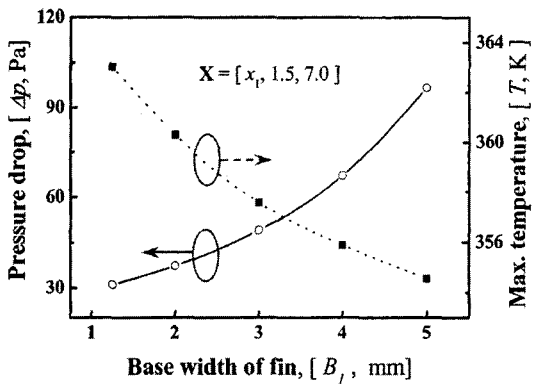

Fig. 4 Effect of base-part fin width on objective functions at $\mathbf{X}=[x_1, 1.5, 7.0]$

To investigate the effect of lower-part fin width (B_2) on the flow and thermal characteristics in the heat sink, the maximum temperature, which is occurred at the bottom surface of second heat source, and the pressure drop between inlet and outlet of heat sink are plotted against various B_2 ($1.25 \leq B_2 \leq 5.0$ mm) and presented in Fig. 5. As can be seen in Fig. 5, the variations of temperature and pressure with increasing B_2 have a similar behavior as B_1, that is, T_j reduces slightly, while ΔP increases linearly as the fin width increases. These are due to the same physical reasons as the effect of B_1. Comparing the Figs. 4 and 5, it is obvious that the influence of B_2 on the thermal and hydraulic performance of heat sink is less significant than that of B_1 (for example, variations of maximum temperature and pressure drop are predicted as 4.46 K and 33.98 Pa, respectively, within the range of B_2, while their variations for B_1 are 8.47 K and 65.48 Pa, as depicted in Fig. 4). Figure 5 also shows that the optimum value of B_2 according to the constraint conditions would be ranged between B_2=1.25 and B_2=3 mm.

The effect of the basement thickness of heat sink (t) on the junction temperature and pressure drop is also investigated and the results are shown in Fig. 6. In contrast with the effects of B_1 and B_2, we can find an interesting phenomenon from the figure. As the basement of heat sink is thickened, the maximum temperature decreases sharply until t=15 mm at which it has a minimum value, and then increases slightly. Heat generated in the heat sink is removed by both conduction and convection. For t>15 mm, more heat would be transferred by conduction through the heat sink. However, as shown in Fig. 6, the maximum temperature is increased on the contrary. This is due to the reduction of heat transfer area which is formed by fins although the flow velocity induced by the fan becomes greater. From this fact, it can be easily found that the convection is more dominant mechanism to enhance heat transfer than the conduction. It can be also seen from Fig. 6 that the pressure drop increases exponentially and the variation of pressure drop is very large in the range of $7 < t < 25$ mm. Comparing with the results of parametric studies, the effect of t on the thermal performance of heat sink is very small compared to other variables, that is, B_1 and B_2.

The parametric studies discussed above show that the fin widths (B_1 and B_2) have a strong influence on the pressure drop and junction temperature in the heat sink, while the effect of base thickness (t) is relatively small. It can be also found in Figs. 4-6 that the objective function simply increases or decreases within the range of design variables. The existence of a unique minimum value for the objective functions, as presented in Fig. 6, indicates that the local optimization technique such as the SQP method becomes an effective optimization algorithm rather than the global optimization.

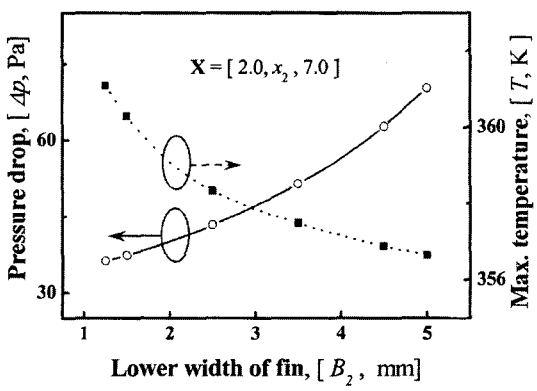

Fig. 5 Effect of lower-part fin width on objective functions at $\mathbf{X}$=[2.0, x_2, 7.0]

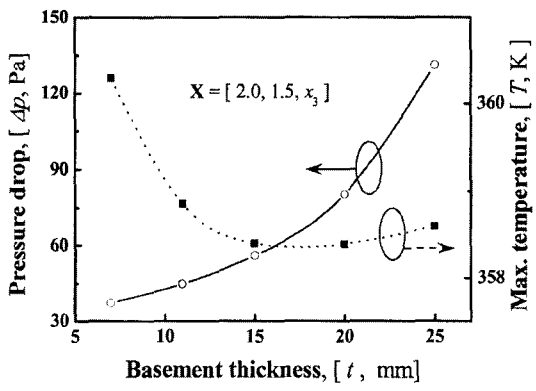

Fig. 6 Effect of basement thickness on objective functions at $\mathbf{X}$=[2.0, 1.5, x_3]

Table 3 Baseline (Initial) and optimized designs for $\Delta T<40$ K

	Baseline	Optimum
Base-part fin width*, B_1	2.0 mm	2.585 mm
Lower-part fin width*, B_2	1.5 mm	1.741 mm
Base plate thickness*, t	7.0 mm	7.914 mm
Fin height, h	53.0 mm	52.086 mm
Thermal resistance (θ_{ja})	0.066 K/W	0.059 K/W
Pressure drop (ΔP)	37.29 Pa	46.72 Pa
Max. junction temperature (T_j)	362.31 K	357.99 K
Temperature rise (ΔT)	44.31 K	39.99 K

5.3 Optimal design

The optimum design variables can be obtained by minimizing the pressure drop subjected to two constraint conditions ($\Delta T<38$ K-41 K and $B_1>B_2$) in the heat sink. In this study, the initial pressure drop for the baseline geometry (ΔP^0) is calculated as 37.29 Pa for $\mathbf{X}_0=[x_1, x_2, x_3; 2.0, 1.5, 7.0]$

Figure 7 shows the convergence histories for two different initial base-part fin widths (i.e., $B_1^0=2.0$ mm and $B_1^0=3.5$ mm) during optimization. In this case, the temperature rise (i.e., one of the constraint conditions) is fixed under 40 K. For two cases, the optimal values of B_1 are obtained as 2.584 mm and 2.581 mm, respectively. From this, it can be found that the same optimal solutions are acquired independent of the initial values. When $B_1^0=3.5$ mm is used as the initial value, there is a sharp decrease initially and the optimal value of B_1 is obtained after about ten iterations. In contrast, in the case of $B_1^0=2.0$ mm, the optimal solution converges within eight iterations. Figure 7 shows that the number of iterations for convergence is usually changed according to the initial values used as well as the constraint conditions. Besides, it can be observed that the number of iterations can be reduced as the initial guessed values of the design variables get close to the optimal values.

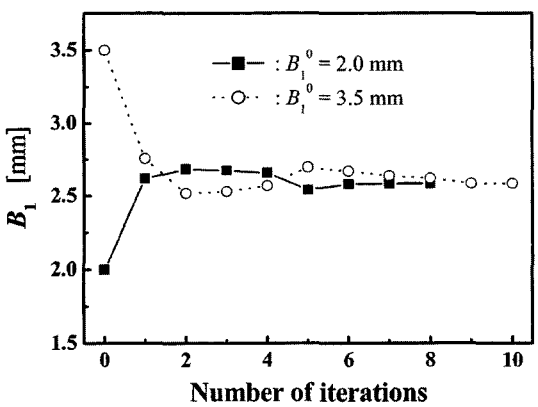

Fig. 7 Convergence histories of base-part fin widths (B_1) for two different initial values

To explain the typical results for optimization, the initial and optimized designs for the temperature rise of 40 K are listed in Table 3. When minimizing the pressure drop in the heat sink, it is important to restrict the temperature rise which is the most important operating factor for the thermal stability of heat sink. As shown in Table 3, the optimized thermal resistance of 0.059 K/W represents a reduction of 10.6% compared to the initial thermal resistance of 0.066 K/W due to the decrease of temperature rise. However, the optimized pressure drop is increased from 37.29 Pa to 46.72 Pa. It can be also seen from Table 3 that the optimal values of all design variables, i.e., the base-part fin width (B_1), lower-part fin width (B_2), and basement thickness (t), are increased compared to those of the initial variables. Especially, B_1 is thickened by 29.25% compared to the initial value as shown in Table 3 and it is obvious that B_1 is the most important variable to enhance the thermal performance of heat sink. This is due to the fact that the velocity in flow passage formed by adjacent fins should increase to reduce the temperature rise (that is, enhance the heat transfer rate) and it results in the increase of pressure drop. The optimized base thickness (t) is extended a little bit (7.0 mm to 7.91 mm). From these results, the base thickness is less significant than other variables for high thermal efficiency of the heat sink.

Table 4 presents the optimum design variables and the corresponding to various results for four different temperature rises, i.e., $\Delta T=38$, 39, 40, and 41 K, and it enables to compare each optimum solution. In Table 4, the "No. of function calls" implies the total number of flow and

Table 4 Optimum designs for various temperature rises

	Baseline	Optimum			
		$\Delta T=38$	$\Delta T=39$	$\Delta T=40$	$\Delta T=41$
Base fin width (B_1)	2.0	3.055	2.816	2.584	2.348
Lower fin width (B_2)	1.5	2.632	2.247	1.741	1.591
Base thickness (t)	7.0	7.767	7.438	7.914	7.579
Fin height (h, $=60.0-t$)	53.0	52.233	52.562	52.086	52.421
Thermal resistance (θ_{ja})	0.066	0.0568	0.0583	0.0598	0.0613
Pressure drop (ΔP)	37.29	62.11	53.36	46.72	41.94
Max.temperature (T_j)	362.31	355.96	356.81	357.99	358.91
No. of iterations	–	13	10	8	4
No. of function calls	–	67	51	42	21

* Unit ; mm for length, K/W for thermal resistance, Pa for pressure drop, and K for temperature

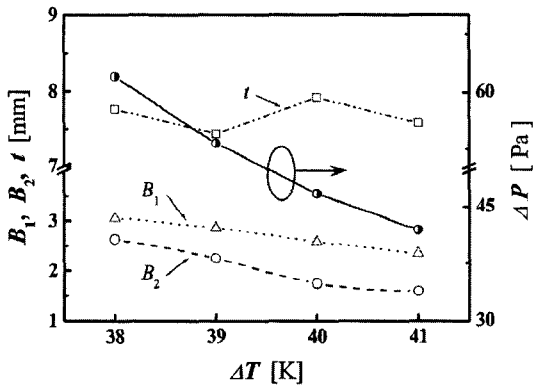

Fig. 8 Optimal solutions for temperature rises

thermal analyses (or total number of changes of design variables proposed by optimizer) required throughout the optimization process. The table illustrates that the more heat is removed, the more iteration for obtaining the optimal solutions is needed (that is, for $\Delta T=38$ and 41 K, the number of iterations are 13 and 4, respectively). On the contrary, if the designer chooses a larger ΔT, the optimizer can easily find the optimal design variables for minimizing the pressure drop during the optimization process. The design variables can be obtained directly from Table 4 for the most useful geometrical configurations of the plate-fins heat sink. This means that if the required temperature rise is 39 K for working in a certain electronic device safely, a designer simply choose the design variables in the second column of optimal results in Table 4. To explain variations of the optimal design variables for four different temperature rises, they are also plotted in Fig. 8 in order to explain easily. It can be observed that the optimum design variables are varied according to the temperature rise (ΔT), as we expected. If the value of required temperature rise is large, the smaller B_1 and B_2 are acquired through the optimization process in order to enhance the heat transfer rate. However, no tendency of the optimized base thicknesses (t) with respect to ΔT is observed. That is, an interesting result is found that the base thickness (t) has maximum and minimum values within the optimal solutions. This arises from the following fact; which the heat transfer mechanism (i.e., conduction and convection) is dominant for a certain temperature rise condition, as discussed in Fig. 6. From this result, it can be noted that the base thickness has little effect on reducing the pressure drop and increasing the thermal performance. Table 4 and Fig. 8 also show that the pressure drop is increased with decrease of ΔT (as the temperature rise is increased from 38 to 41 K, the pressure drop is reduced by 32.2% (i.e., it is decreased from 62.11 to 41.94 Pa. Note that these values are increased by 66.5 and 12.5% compared to the baseline condition), while the thermal resistance is increased from 0.0568 to 0.0613 K/W. This clearly shows that for the design of the heat sink with plate-fins, it is very

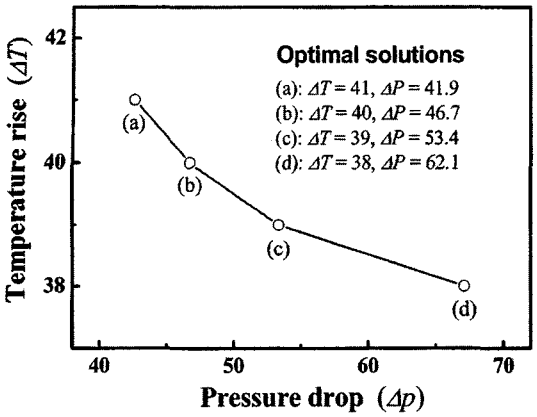

Fig. 9 Relationship between temperature rise (ΔT) and pressure drop (ΔP)

important to choose the proper design parameters by considering which one is preferable between the pressure drop and the thermal resistance (or temperature rise).

A set of optimal solutions for the objective function can be constructed so that the designer can select the preferred solution based on Table 4. For this purpose, the relationship between the pressure drop (Δp) and the temperature rise (ΔT) is illustrated in Fig. 9. The points on the curve from (a) to (d) are one of the optimal solutions. The results can be very helpful to designers in order to achieve the optimization of the heat sink. For example, when designers want to focus on decreasing the thermal resistance rather than decreasing the pressure drop, they can select the points such as (c) or (d) on the curve of Fig. 9 and then read the corresponding optimal design variables in Table 4. For the thermal management of the heat sink, it is important to remark that the most important goal is to maximize the heat transfer rate or minimize the thermal resistance and this is easily achieved by the increase of the velocity between fins and the heat transfer area, as discussed in Figs. 5~7. However, the minimized pressure drop is strongly related to the specific cost, because the pressure drop determines the size of the fan needed to blow the cool air through the channel. Therefore, choosing one of the optimal solutions in Fig. 9 is dependent on the heat sink designers.

6. Conclusions

We numerically obtained the optimum design variables of a plate-fins heat sink to minimize the thermal resistance between the heat source and heat sink and the pressure drop in the heat sink. The thermal and flow characteristics in the heat sink were analyzed using the finite volume method. And the SQP method, which is one of the local optimization techniques, was used for solving the constrained optimization problem. As the results of optimization, the following conclusions were obtained:

A use of vortex generator in the heat sink was one of the effective tools to improve the thermal performance. The most dominant design variables for the pressure drop and thermal resistance were the base-part fin width (B_1), and the lower-part fin width (B_2), while the effect of base thickness (t) on them was relatively small compared to the other two design variables. The optimal design variables could obtain by the integration of CFD code and local optimization technique which is one of the mathematical optimization techniques. The accuracy of optimal results was validated through the optimization process for two different initial values of B_1. The results also showed that the optimal design variables for the temperature rise of 40 K were as follows: B_1=2.584 mm, B_2=1.741 mm, and t=7.914 mm. In this case, the thermal resistance for the optimum model was decreased by 10.1%, while the pressure drop was increased by 25.3% compared to those of the baseline model. It was also found that the optimal design variables were varied with the desired temperature rise which is the most important factor for the thermal stability of heat sink. The optimization could be completed as the optimal solutions were plotted for the relationship between pressure drop and temperature rise. The results of this work can offer designers the information they need to select the optimal design variables corresponding to the preferred objective functions.

Acknowledgment

This research was supported by The Center of Innovative Design Optimization Technology (iDOT), Korea Science and Engineering Foundation.

References

Abe, K., Kondoh, T. and Nagano, Y., 1996, "A Two-Equation Heat Transfer Model Reflecting Second-Moment Closures for Wall and Free Turbulent Flows," *Int. J. Heat and Flow Flow*, Vol. 17, pp. 228~237.

FLUENT 5 User's Guide, FLUENT Inc., 1998.

Jang, J. Y., Wu, M. C. and Chang, W. J. 1996, "Numerical and Experimental Studied of Three-Dimensional Plate-Fin and Tube exchangers," *Int. J. Heat Mass Transfer*, Vol. 39, No. 14, pp. 3057~3066.

Ledezma, G. and Bejan, A., 1996, "Heat Sinks with Sloped Plate Fins in Natural and Forced convection," *Int. J. Heat Mass Transfer*, Vol. 39, No. 9, pp. 1773~1783.

Ma, H. B. and Peterson, G. P., 2002, "The Influence of the Thermal Conductivity on the Heat Transfer Performance in a Heat Sink," *ASME J. of Electronic Packaging*, Vol. 124, pp. 164~169.

Park, K., Choi, D. H. and Lee, K. S., 2004, "Design Optimization of Plate-Fin and Tube Heat Exchanger," *Numerical Heat Transfer Part A*, Vol. 45, pp. 347~361.

Patankar, S. V., 1980, *Numerical Heat Transfer and Fluid Flow*, Hemisphere, Washington.

Rodi, W., 1984, *Turbulence Models and Their Applications in Hydraulics a State-Art-of Review*, Book Publication of International Association for Hydraulic Research, Delft, Netherlands.

Ryu, J. H., Choi, D. H., and Kim, S. J., 2003, "Three-Dimensional Numerical Optimization of a Manifold Micro Channel Heat Sink," *Int. J. Heat Mass Transfer*, Vol. 46, pp. 1553~1562.

Vanderplaats, G. N., 1984, *Numerical Optimization Techniques for Engineering Design with Application*, Chap. 2, McGraw-Hill, New York.

Wirtz, R. A. and Zcheng, N., 1998, *Methodology for Predicting Pin-Fin Fan-Sink Assembly Performance, Prodc. of 6th InterSociety Conference on Thermal and Thermomechanical Phenomena in Electronic Syatems (Itherm '98)*, S.H. Bhavnani et al., ed., pp. 303~309.

Wong, T., Leung, V. W., Li, Z. Y. and Tao, W. Q., 2003, "Turbulent Convection of Air-Cooled Rectangular Duct with Surface-Mounted Cross-Ribs," *Int. J. Heat Mass Transfer*, Vol. 46, pp. 4629~4638.

Yuan, Z. X., Tao, W. and Wang, Q., 1998, "Numerical Prediction for Laminar Forced Convection Heat Transfer in Parallel-Plate Channel with Streamwise-Periodic Rod Disturbances," *Int. J. of Numerical Methods in Fluids*, Vol. 28, pp. 1371~1387.